Nuclear Instruments and Methods 171 (1980) 529–534

A CYCLIC TIME OPTIMIZATION APPROACH TO THE STUDY OF ^{252}Cf FISSION PRODUCTS

R.I. PRICE *, I.D.U. EBONG, John A. ADAMS ** and R.R. ROY
Department of Physics, Arizona State University, Tempe, Arizona 85281, USA

Received 7 August 1979 and in revised form 20 November 1979

A K X-ray-beta particle coincidence technique has been investigated for the study of the beta decay of fission products from ^{252}Cf. A fission-fragments transport system has been developed and its optimization curve used for the identification of the half-life associated with the K X-ray peak originating from the Mo → Tc decay. A high-resolution lithium-drifted silicon spectrometer and a plastic scintillation spectrometer were used in the analysis of the K X-rays and beta particles repsectively. A half-life of (0.98 ± 0.03) min was associated with the K X-rays from technetium. A Kurie plot of the coincidence beta spectrum revealed at least three beta groups with end-point energies of (2.19 ± 0.19) MeV, (1.64 ± 0.14) MeV and (1.04 ± 0.10) MeV.

1. Introduction

In recent years, rapid chemical separation techniques or magnetic isotope separators, on-line to reactors, have been employed to study the beta activity of the neutron-rich, intermediate mass nuclei formed in the fission process. The studies have been difficult because of the need to separate the desired nucleus from the multitude of other nuclei produced in fission.

An alternative approach to this problem is to measure the beta decay of the selected fission fragment, using a plastic scintillation spectrometer, in coincidence with a K X-ray from the beta decay daughter nucleus. This K X-ray coincidence technique which has been used in the present experiment, as in previous studies [1–3], allows the assignment of the atomic number Z to the neutron-rich isotope which undergoes beta decay, provided that the beta decay is not to a long-lived metastable state of the daughter. The use of this technique allows the beta decay of some of the neutron-rich fission fragments to be studied without the need to chemically separate the elements.

The use of the plastic scintillator spectrometer for beta studies offers some advantages over other methods: (1) when used with a multichannel pulse-height analyzer, the entire energy spectrum can be recorded during a counting interval; (2) its small physical dimensions and low-cost make it an attractive alternative instrument; and (3) the high detection efficiency ability makes it a desirable instrument when used in coincidence studies. The most severe drawback of the scintillator beta-ray spectrometer is its inherently poor energy resolution and considerable backscatter.

Freedman et al. [4] published one of the first attempts to correct the beta-ray energy spectrum, obtained with a scintillator for resolution and backscatter effects. The basic response of an organic scintillator to monoenergetic electrons, consists generally of a Gaussian peak centered about the full energy, and a tail which arises from partial energy loss due to scatter from the crystal [5]. Over the years, various other methods have been used to correct for response functions of measurement devices [6–17]. The method used here to correct for the response function is described in Appendix 1.

In the present experiment we investigate the feasibility of using the K X-ray and beta particle coincidence techniques to obtain the beta spectrum and the end-point energy of a neutron-rich isotope formed in the fission of californium-252. In addition a method will also be described to determine the half-life of a beta emitter formed in the fission.

2. Experimental detail and procedure

The technique involved cycles of collection of fission fragments in a Mylar tape, transportation of the

* Present address: Physics Department, Kearney State College, Kearney, Nebraska 68847 USA.
** Present address: IRT Corporation, 7650 Convoy Court, PO Box 80817, San Diego, CA 92138 USA.

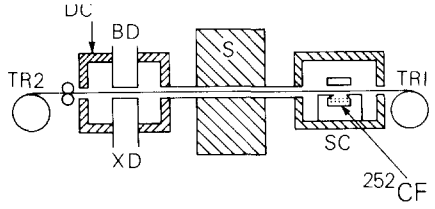

Fig. 1. Experimental arrangement. (TRI) tape reel: (SC) source chamber; (S) shielding; (BD) beta particle detector; (XD) X-ray detector; (DC) detection chamber (TR2) tape reel.

fragments to the counting position, and an X-ray coincidence counting of the beta particles from the fission products. The fission fragments source, obtained from the Oak Ridge National Laboratory, was a thin deposit of 0.7 μg of californium oxychloride on an aluminium disk. It was covered with a thin colloidal substance, which served to keep the californium from migrating and yet was thin enough to allow the fragments to be ejected through it. The initial activity was of the order of 10^5 fissions per minute.

The experimental set-up is shown in fig. 1. The tape from the reel TR1 was passed directly over the source in the chamber SC, and through a guide in the shielding S into the detection chamber DC. In the detection chamber it was passed between the electron and the X-ray detectors. From this chamber the tape was passed through two pinch rollers, driven by a microprocessor controlled precision stepping motor, and placed on reel TR2. The source-to-detectors distance measured 1.4 m and the shielding material used in this space sufficiently eliminated stray radiations from the source chamber.

Over the source position a shutter was built between the tape and the source. Above the tape a plunger was built. Both the shutter and the plunger were electronically controlled by the microprocessor (SWT 6800) which executed the collection and transportation phases of the experiment. The shutter was opened for fragment collection during the collection interval and closed during the transportation interval, while the plunger was lowered, to serve as a source seal, during the collection interval and raised during the transport interval.

A Si(Li) Kevex detector was used for X-ray detection while a modified commercial organic scintillator, Pilot B, with an Ortec Photomultiplier and base were used for the electron detection. Fig. 2 shows the electronics set-up. Branch A of this arrangement was used for the cycle optimization time which is described later in this section. It is the self-grating circuit used for selecting the window width for the X-ray of the element under study. The X-ray energy calibration was performed by using Mo, Co, Ti, Zr, Ag, Zn, In, Ba and Pd X-rays sources. The resolution was 0.88 kev at 32 kev.

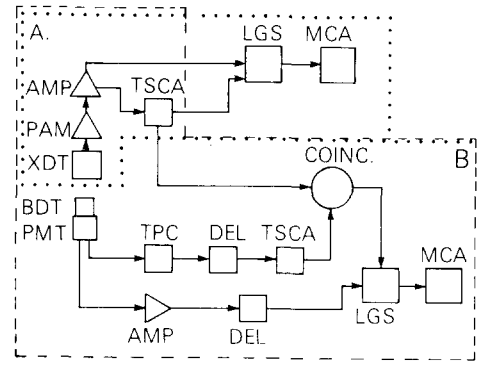

Fig. 2. Block diagram of the electronics. (BDT) beta particle detector (scintillator: (PMT) photomultiplier tube; (XDT) X-ray detector; (PAM) preamplifier; (AMP) amplifier; (TSCA) time single channel analyzer (LGS) linear gate and stretcher; (COINC) coincidence unit; (TPC) time pick-off control; (DEL) delay amplifier; (MCA) multichannel analyzer.

The beta detector was calibrated in the ungated mode of the linear gate and stretcher in branch B, using the standard beta sources ^{90}Y, ^{147}Pm, ^{36}Cl and the conversion electron line in ^{137}Cs. The FWHM was 100 keV at 0.626 MeV. (The calibration curve was linear up to 2.3 MeV.)

The beta spectrum was obtained by first requiring coincidence between the X-ray signals from the time single-channel analyzer (TSCA) and the electron timing signal from the time pick-off control. The resulting signal from the universal coincidence unit was used as a gating signal for the electron signal arriving at the linear gate and stretcher.

Cycle optimization: for a given radioactive element in the collected fragments, it was observed that the count rate at the X-ray detector varied with the collection and counting times per cycle. It was therefore necessary to obtain an optimum collection/counting time schedule for efficient operation of the experiment.

The cycle optimization procedure employed is based on the continuum theory of radioactivity and as such is similar in principle to that reported in refs. [18], [19] and [22]. Three time periods recognized for each counting cycle were t_1, time for the build-up and decay of the radioactive nuclide (fragments collection time); t_2, source to detectors trans-

port time; t_3, detector counting time. The total number of counts recorded in a detector for each cycle is given by

$$N_D = KEB(t_1)\,T(t_2)\,D(t_3)\,, \qquad (1)$$

where * K = (production rate)/(decay constant); E = detection efficiency involving a geometrical factor; $B(t_1)$, $T(t_2)$, $D(t_3)$ are respectively build-up, transport, and counting factors given by:

$$B(t_1) = 1 - \exp(-\lambda t_1)\,,$$

$$T(t_2) = \exp(-\lambda t_2)\,,$$

$$D(t_3) = 1 - \exp(-\lambda t_3)\,,$$

and λ is the decay constant of the nuclide under study. The foregoing factors are valid only for the case in which the parent's half-life is short compared with the daughter's half-life.

At the end of n cycles, involving a total counting time $T_0 = nt_3$, the total of the accumulated counts is

$$N_{DT} = nN_D = nEKT(t_2)\,B(t_1)\,D(t_3)$$

$$= \frac{T_0 EK}{t_3}\,T(t_2)\,B(t_1)\,D(t_3)\,. \qquad (2)$$

With the following conditions (which applied in this experiment):

(a) $t_1 = t_3 = t$:

i.e.,

$$B(t_1)\,D(t_3) = B(t)\,D(t) = [B(t)]^2$$

and

(b) t_2 = constant :

i.e.,

$T(t_2)$ = constant ,

eq. (2) becomes

$$N_{DT} = \frac{P}{t}\,[B(t)]^2 = \frac{P}{t}\,[1 - \exp(-\lambda t)]^2\,, \qquad (3)$$

where

$P = EKT_0 \exp(-\lambda t_2)$ = constant for a given element .

It can be easily shown that N_{DT} has a maximum at $t = t_m$ where

$$t_m = 1.8128 T_{1/2} = 1.2565/\lambda\,. \qquad (4)$$

If the half-life of the parent is greater than 10% of that of the daughter, the value for t_n in eq. (4) will be in error by more than 4%. The error in the single component assumption of eq. (4) can be radily estimated by considering the effects of the parent's and grandparent's half-lives.

Hence when the experiment was carried out for a different cycle time t, a peak cycle time t_m was obtained. From this, the half-life of the decay was established. Fig. 3 shows the optimization curve obtained in this experiment. This procedure also provides a method of estimating the percentage overlap from neighboring Kβ X-ray peaks. In many cases the difference in half-life between these neighboring elements meant that this cycle optimization procedure also minimized such overlap thereby providing a definite Z identification for the nuclide. For isotopes of the same Z value the difference in half-lives implies different t_m values.

The data obtained in the experiments (fig. 3) were

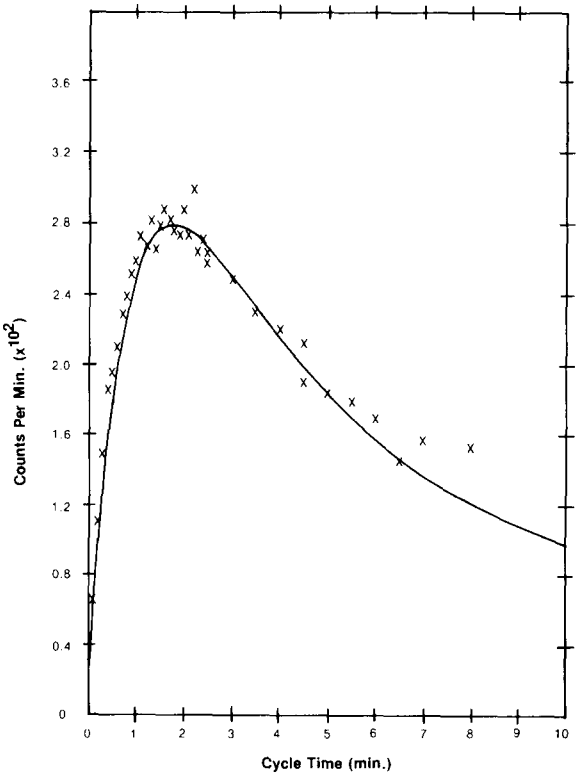

Fig. 3. Cycle optimization curve. Continuous curve shows the theoretical fit to the experiment points.

* The time dependence of K is ignored here because the total data collection time T is very small compared with the mean life of the fissioning nucleus.

fitted to the theoretical curve given by eq. (3), by the method of least squares fitting.

3. Results and discussion

The beta particles emitted from a particular fission fragment were measured in coincidence with K X-rays emitted by the daughter products. This enabled us to identify the element which decayed by the emission of beta particles. The end point energy E_0 of the beta spectrum was obtained from the Kurie plot.

$$K(E) = [N(E)/F(Z, E)\, C_n PE]^{1/2} \text{ versus } E ,$$

where $N(E)$ = the number of beta particles with energy E after correcting for backscattering (see Appendix 1); $F(Z, E)$ = Fermi function; C_n = Matrix shape factor; P = momentum of a beta particle; and E = total relativistic energy of a beta particle.

A linear least-squares fit was used to obtain the end-point energies of the Kurie plot. A χ^2 test was used to check the fit. For ease in checking the regions of discrepancy at low energy and towards the end-point energies, a theoretical spectrum was generated using the end-point energies and compared with the normalized beta spectrum obtained in the experiment. The theoretical spectrum depends on the end-point energy and the shape factor C_n. The corrected beta spectrum shown in fig. 4 with a total of 1.033 X 10^5 events, was obtained using technetium K X-rays as gates for the beta particles. This implies that the observed decays were from molybdenum nuclides. From the optimization curve (fig. 3) the half-life obtained for the decaying nuclide was (0.98 ± 0.03) min. Three beta groups were identified from the beta spectrum of fig. 4. The end-point energies (see fig. 5) were (2.19 ± 0.19) MeV, (1.64 ± 0.14) MeV and (1.04 ± 0.10) MeV and the relative intensities were 62.4%, 29.7% and 7.9% respectively. These values were obtained from a least-squares fit of the sum of the theoretical spectra to the observed spectrum. The peaks A, B, and C in fig. 4 are thought to be due to conversion electrons originating from the deexcitation of ^{104}Tc. This interpretation is consistent with the value of approximately 2.4 MeV, which we have measured experimentally, for the total transition energy available for the Mo → Tc decay. The conversion peak A is associated with the highest end-point energy, 2.19 MeV. The peaks B and C are respectively associated with the end-point energies 1.64 MeV and 1.04 MeV.

The nuclides ^{103}Mo and ^{104}Mo have about the same half-life [23] as measured in this experiment. However the measured half-life ($T_{1/2} \geqslant 18$ min) of Tc, formed in the Mo → Tc → Ru chain, is greater than that associated with the ^{103}Tc → ^{103}Ru decay. This implies that the decaying nuclide is ^{104}Mo.

The beta–X-ray coincidence technique used in this experiment is complimentary to the beta–gamma coincidence technique which has been frequently used in the investigation of beta decay of fission fragments [20–21]. The beta–X-ray coincidence technique is useful for those beta particle groups which decay leading to excited states and in which the daughter nuclei de-excite with high conversion probabilities.

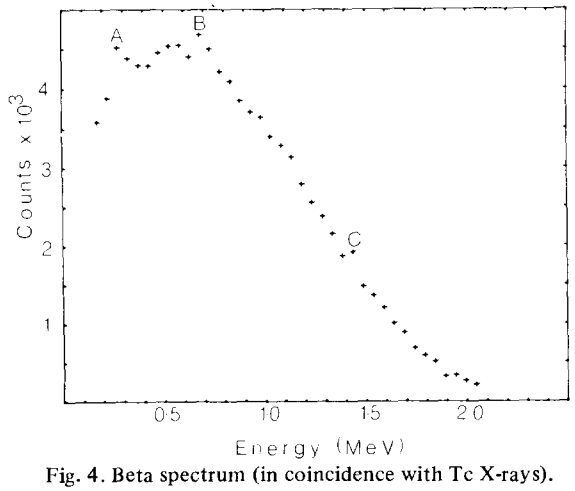

Fig. 4. Beta spectrum (in coincidence with Tc X-rays).

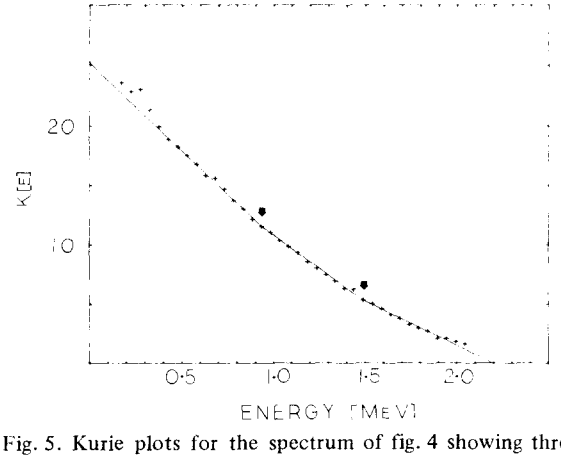

Fig. 5. Kurie plots for the spectrum of fig. 4 showing three beta groups. Arrow indicates change in slope.

Appendix 1: derivation of backscattering correction

The procedure used for the correction of the backscattering effect is similar to the method reported by Charoenkwan [10]. However, an important correction was made to the derivation in ref. [10]. The response of the beta detector used in this experiment, to a conversion electron line, was a Gaussian distribution centered at the energy of the line and a flat tail in the lower energy region. A constant backscattering coefficient P independent of the primary electron energy was assumed. Experimentally, P was obtained as the ratio of the area under the tail to the total area under the observed response. The correction formalism was developed as follows:

At the energy E_1 in the range of the observed spectrum, for unit time, let: $N_i(E)$ = number of primary electrons incident on detector with energy between E and $E + \Delta E$; $N_b(E)$ = number of electrons backscattered from higher energies to energies between E and $E + \Delta E$; $N_f(E)$ = number of electrons backscattered from the energy interval between E and $E + \Delta E$ to lower energies; $N_d(E)$ = number of electrons detected in the interval E and $E + \Delta E$. The primary number per unit time arriving at the detector, i.e., $N_i(E)$, can thus be represented by

$$N_i(E) = N_d(E) + N_f(E) - N_b(E) . \tag{A1}$$

By definition

$$P = N_f(E)/N_i(E) .$$

Substituting in eq. (A1) the following is obtained

$$(1 - P) N_i(E) = N_d(E) - N_b(E) . \tag{A2}$$

For the last energy interval (about the end-point energy E_0) $N_b(E_0) = 0$, therefore from eq. (A2)

$$N_i(E_0) = [1/(1 - P)] N_d(E_0) .$$

For the next energy interval centered at $E = E_0 - \Delta E$, $N_b(E_0 - \Delta E)$ are all due to backscattering from $N_i(E_0)$. If the backscattering tail is flat, as was indeed the case, then the backscattered electrons from the energy interval about E_0, i.e., from $N_i(E_0)$, are equally distributed into all intervals between 0 and E_0. Therefore the contributions to $N_b(E_0 - \Delta E)$ from $N_i(E_0)$ is

$$\frac{PN_i(E_0)}{(E_0 - \Delta E)/\Delta E} = N_b(E_0 - \Delta E) . \tag{A3}$$

From eq. (A2) it follows that

$$N_i(E_0 - \Delta E) = \left(\frac{1}{1 - P}\right)\left(N_d(E_0 - \Delta E) - \frac{PN_i(E_0)}{(E_0 - \Delta E)/\Delta E}\right) .$$

The backscattering contributions in the interval about $E_0 - 2\Delta E$ are from the intervals about E_0 and $E_0 - \Delta E$. Using similar arguments as those preceding eq. AI-3, this correction is given by

$$N_b(E_0 - 2\,\Delta E) = \frac{PN_i(E_0)}{(E_0 - \Delta E)/\Delta E} + \frac{PN_i(E_0 - \Delta E)}{(E_0 - 2\,\Delta E)/\Delta E} = P\,\Delta E\left(\frac{N_i(E_0)}{E_0 - \Delta E} + \frac{N_i(E_0 - \Delta E)}{E_0 - 2\,\Delta E}\right) .$$

Therefore

$$N_i(E_0 - 2\,\Delta E) = \left(\frac{1}{1 - P}\right)\left[N_d(E_0 - 2\,\Delta E) - P\,\Delta E\left(\frac{N_i(E_0)}{E_0 - \Delta E} + \frac{N_i(E_0 - \Delta E)}{E_0 - 2\,\Delta E}\right)\right] . \tag{A4}$$

Similarly it follows that the number of primary electrons per unit time in the energy interval about $E_0 - n\Delta E$ is given by

$$N_i(E_0 - n\,\Delta E) = \left(\frac{1}{1 - P}\right)\left(N_d(E_0 - n\,\Delta E) - P\,\Delta E \sum_{m=1}^{n} \frac{N_i(E_0 - (m - 1)\,\Delta E)}{(E_0 - m\,\Delta E)}\right) .$$

The $[1/(1 - P)]$ factor in the first term is missing from ref. [10].

This formalism was applied to the 0.626 MeV conversion line from the transition ^{137}Cs β ^{137}Ba. The conversion electrons were detected in coincidence with K X-rays of ^{137}Ba. The flat tail was satisfactorily removed. The resulting distribution was essentially Gaussian with a total area under the distribution equal to the total area under the previous uncorrected response curve.

After the backscattering effect has been corrected for, the "continuous" beta spectrum is now primarily affected by the Gaussian response, as demonstrated in the case of the conversion electron line. Kennett and Keech [7] have shown that such a Gaussian response to monoenergetic electrons may be replaced with a delta function response without serious effects to the linearity of the Fermi–Kurie plot for beta decay.

Noticeable effects are expected only at the very extremes of the plot, without appreciable error in the determination of the end-point energy.

This technique has been applied to the well known case of ^{90}Y and was found to be valid.

References

[1] D.R. Ruegsegger, Jr. and R.R. Roy, Phys. Rev. C1 (1970) 632.
[2] N.W. Eddy and R.R. Roy, Phys. Rev. C3 (1971) 878.
[3] V.V. Skliarevskii, D.E. Fomenko and E.P. Stepanov, J. Exp. Theor. Phys. (USSR) 32 (1957) 256.
[4] M.S. Freedman, T.B. Novey, F.T. Porter and F. Wagner, Rev. Sci. Instr. 27 (1958) 716.
[5] I.S. Sherman, M.S. Freedman, F.T. Porter and F. Wagner, Jr., IEEE Trans. Nucl. Sci. NS11 (1964) 20.
[6] H.E. Bosch and T. Urstein, Nucl. Instr. and Meth. 24 (1963) 109.
[7] T.J. Kennett and G.L. Keech, Nucl. Instr. and Meth. 24 (1963) 142.
[8] B. Persson, Nucl. Instr. and Meth. 27 (1964) 1.
[9] G. Bertolini, F. Cappellani, R. Fautechi and G. Restelli, Nucl. Instr. and Meth. 27 (1964) 281.
[10] P. Charoenkwan, Nucl. Instr. and Meth. 34 (1965) 93.
[11] F.T. Porter, M.S. Freedman, F. Wagner, Jr. and I.S. Sherman, Nucl. Instr. and Meth. 39 (1966) 35.
[12] J.Mc L. Emmerson, Nucl. Instr. and Meth. 40 (1966) 163.
[13] P. Sen and A.P. Patro, Nucl. Instr. and Meth. 40 (1966) 1.
[14] J.T. Grissom, D.R. Koehler and B.G. Gibbs, Nucl. Instr. and Meth. 45 (1966) 190.
[15] R.H. Richie and V.E. Anderson, Nucl. Instr. and Meth. 45 (1966) 277.
[16] E. Jacobs, L. Dorikens-Vanpraet, J. Demuynck and D. de Frenne, Nucl. Instr. and Meth. 47 (1967) 55.
[17] D.D. Slavinskas, T.J. Kennet and W.V. Prestich, Nucl. Instr. and Meth. 37 (1967) 36.
[18] M. Wiernik and S. Amiel, Modern trends in activation analysis, (NBS Spec. Publ. 312) p. 929.
[19] K.W. Macmurdo and W.W. Bowman, Nucl Instr. 141 (1977) 299.
[20] F.K. Wohn and W.L. Talbert, Jr., Phys. Rev. C18 (1978) 2328.
[21] F.K. Wohn, K.D. Wunsch, H. Wollink, R. Decker, G. Jung, E. Kogbin and G. Siegert, Phys. Rev. C17 (1978) 2185.
[22] J.B. Wilhelmy, Univ. of California, Lawrence Radiation Lab. Report UCRL-18978 (1969).
[23] C.M. Lederer and V.S. Shirley, Table of isotopes 7th ed. John Wiley, New York, 1978).